International Journal of Ecology and Environmental Sciences
www.ecologyjournal.in
Online ISSN: 2664-7133; Print ISSN: 2664-7125
Received: 10-02-2019; Accepted: 13-03-2019
Volume 1; Issue 2; April 2019; Page No. 32-46

Urban growth assessment and its impact on deforestation in makurdi metropolis, Nigeria

Jande JA[1*], Nsofor GN[2], Mohammed M[3]
[1] Department of Social and Environmental Forestry, Federal University of Agriculture Makurdi, Makurdi, Benue State, Nigeria
[2-3] Department of Geography, Federal University of Technology, Minna, Niger State, Nigeria

Abstract
There has been a rapid growth of urban areas across the globe since 1950s with the majority of world population living in urban areas, in search of better job opportunities and services. This trend of transition from rural to urban is expected to continue to rise and government in developing countries are likely going to face more challenges in different sectors, necessitating the need of understanding the spatial pattern of the growth and its impact on the environment for an effective urban planning. The study was aimed at modelling urban growth in Makurdi and the impacts on deforestation The study covered a period of 30 years; from 1987 to 2017, and the major transitions to urban were modelled to predict the future scenarios in 2030. Three Landsat satellite images of 1987, 2007 and 2017 were classified using maximum likelihood classifier in Idrisi Selva to detect the land cover changes and a classification overall accuracy was 88.78%, 82.7% and 80.52% for 1987, 2007 and 2017 maps while Kappa index of agreement (KIA) was 0.86. 0.79 And 0.76 for the same period. The result of the classification revealed that between 1987 and 2017, urban area in Makurdi increased to the tune of 12125ha (422.33%) at the rate of 14.07% while forest declined by 11742ha (52.21%) at the rate of 1.74%. Physical and proximity factors such as distance from urban areas, distance from roads, distance from rivers, elevation, slope, population density, evidence likelihood of transition and distance from railways were identified as major factors driving urban growth in the area. It was found that evidence likelihood of transition and the distance from urban areas and distance from railway were the most important factors shaping urban growth in the area. Thereafter, a Multilayer Perceptron Markov (MLP-Markov) model was used to model transition potentials of various LULC types to predict future changes. The models had a reliability of 81.4%, after validation. The results of the prediction show that urban area will increase from 17.95% to 20.81% while forest will decline from 12.85% to 10.25% during the period and that urban area is the third largest contributor to deforestation. It reveals that Makurdi will grow at the rate of 2.86. Analysis of the prediction revealed that the rate of urban growth will continue and would certainly threaten forest areas in the area. Makurdi stands the risk of extreme deforestation if appropriate measures are not taken.

Keywords: land use and land cover, urban growth, modelling, deforestation, idrisi selva, KIA, makurdi and mlp-markov

1. Introduction
Today, urban growth is one of the most important issues in Africa. According to the prediction of the United Nations, the population of Africa will double within the next 40 years: from about 1 billion in 2010, Africa is expected to reach 2 billion inhabitants around 2045. Present urban growth in Africa is driven by both high natural growth rates and the concurrent rural-urban migration (UN, 2014). Most of this rapid urbanization will take place on agricultural land, vegetation and other natural land cover. It is shown that the rate of urban physical expansion is much faster than urban population growth in many cities which is often referred to as urban sprawl, presenting the increasing pressure on land resources. The increasing scarcity of limited land resources due to anthropogenic activities – particularly by urban growth – has not been given enough attention, which poses a great challenge to achieve the goals of sustainable development Urban areas are expanding at a very rapid rate the world over (Al-shalabi, *et al*, 2012) [4]. This urban expansion is creating a lot of challenges in many countries especially developing countries in terms of deforestation and land degradation (Musa *et al*, 2017) [23]. According to the United Nations (UN, 2014), urban areas are housing more people now compared to rural areas In spite of the fact that urbanization remains a key to modernization, economic growth and development, it equally has some side effects on the environment (Xie and Fan, 2014) [37]. The remarkable population growth adds to the ever-increasing pressure on urban land supply with profound environmental implications. Inadequate housing and infrastructure, slum proliferation, haphazard land development, incessant flooding, widespread poverty and unemployment are among the major issues of unsustainable urban growth requiring the intervention of town planners and decision makers (Okwuashi, 2011) [27]. The growth and development of urban areas has a lot of influence on deforestation and therefore calls for an investigation into the nature of their growth and the impacts on the physical environment especially in terms of biodiversity and land degradation.

Several studies have revealed that the integrated Multi-Layer Perceptron-Markov chain (MLP-MC) method is a robust tool to quantify and model the spatio-temporal LULC changes that combines remote sensing and GIS efficiently (Ahmed et al., 2013; Mishra, Rai, & Mohan, 2014; Ozturk, 2015) [3, 22, 28]. In the last 20 years, remote sensing (RS) and geographical information systems (GIS) have been acknowledged as powerful and effective tools for the management of land and other natural resources. These technologies have proved their efficacy for updating and

managing spatial data in developing countries by providing the advantage for rapid data acquisition to collect LULC information regularly at a much lower cost than traditional ground survey methods. The application of RS and GIS in urban and environmental planning has led to the formation of spatial modeling methods including MLP-MC

Several studies have been carried out to assess urban growth in the past (Ebrahimipour *et al*, 2016; Hegazy and Kaloop, 2015; Zhang, 2016) [13, 16, 38] and its impact on the environment, only very few have been directed at assessing the impacts of urban growth on deforestation such as Danburi, 2015; Eltom *et al*, 2013; Hussaini, 2014; and Musa et al., 2017 [11, 14, 20, 23]. In areas where deforestation is taking place as in the case of Makurdi metropolis, decision making for proper environmental management strategy would require knowledge of the magnitude of the deforestation and where it has taken place but this remains a challenging issue (Musa et al., 2017) [23].

It has been observed that Makurdi has witnessed an accelerated expansion of infrastructure like the new housing schemes and layouts, opening of roads, building of new markets with the reintroduction of democratic rule in 1999. This has led to expansion such that all the hitherto rural villages such as Agan, Tse-Ayu, Terwase Agbadu, Nyiman, Kanshio, Apir and Fiidi amongst others have been engulfed by the spatial extension of the city's boundaries. Although this observation reveals the typical growth characteristics of infill, expansion and outlying, no sufficient empirical evidence of this growth has been published. (Hemba, *et al*, 2017) [17] This study therefore seeks the use of remote sensing and Geographic Information System (GIS) techniques in assessing urban growth and its impacts on deforestation in Makurdi metropolis, Makurdi.

There is no doubt that modeling the urban land use dynamics of Makurdi requires the employment of robust techniques and tools that can model the growth, complexity and dynamics of the town. The objective of this study is to analyze and simulate LULC changes in Makurdi Metropolis from 1987 to 2017 and then predict scenarios of future LULC changes quantitatively and spatially for 2030 based on MLP-MCA methods and its implications for deforestation.

2 Materials and Methods

2.1 Study Area

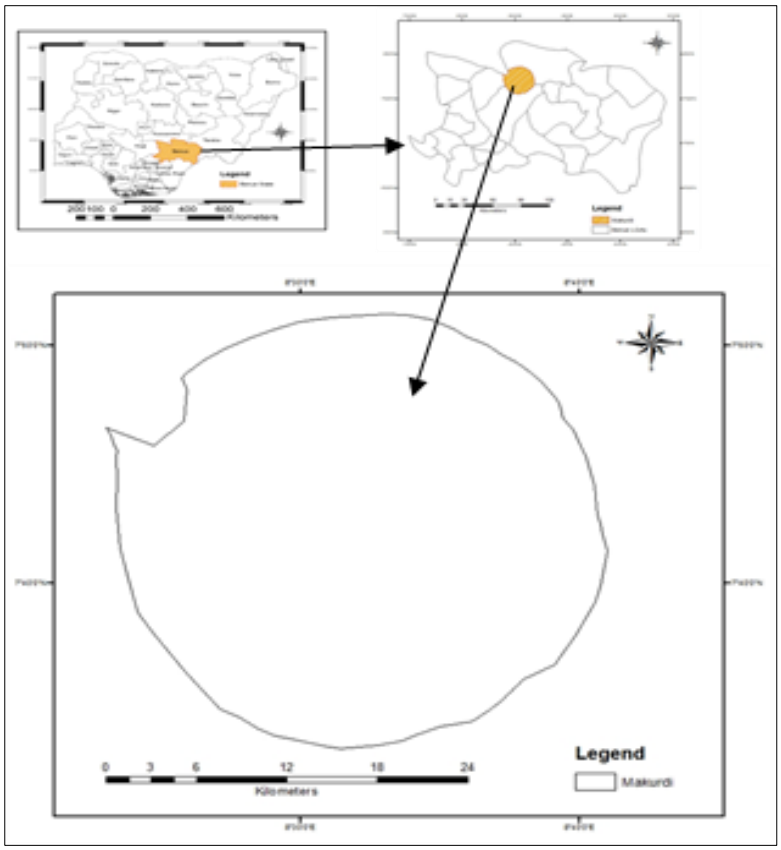

Fig 1: Map of Study Area.

Makurdi the Benue State capital is located in the north central Nigeria. The city is located between longitude 8^0 24′ E and $8^0$38′ E of the Greenwich Meridian and latitude 7^0 38′ N -7^o 50′ N, of the equator (Figure1). It is traversed by a major tributary of River Niger, the second largest river in the country, the River Benue. The town is divided into two major blocks by River Benue hence the North and South banks. It has a population of 300, 377 according to the 2006 population. Makurdi has a unique shape in the whole country with a circular radius of 16km. The city, which started as a small river port in 1920 and later became a Colonial Provincial headquarter in 1927.Makurdi is currently subdivided into eleven council ward namely; Agan, Bar, Fiidi, Central South

Mission, Clerk/Market, Mbalagh, Modern Market, North Bank 1, North Bank 2, Wadata/Ankpa and Wailomayo (Abah, 2014) [1].

Makurdi is located in the tropical climate region and has two different seasons, the rainy (wet) season and the dry season (Abah, 2014) [1]. The wet season commences in the month of April and lasts till October having a break in August, while the dry season starts from November and ends in March. The yearly rainfall is between 15cm and 18cm. Temperatures varies between 23^0C-38^0C for most of the year. According to the classification by Thornthwaite, the area is represented as *B3* (Humid climate with seasonal distribution of moisture). The mean monthly values of rainfall in the area range from 0.77cm to 22.75cm. This has brought about three distinct rainfall periods in the area: the wet period, the moderate period and the dry period. The harmattan winds usually brings a cooling effect particularly from November to February and it is linked with seasonal dust haze coming from the prevailing dry NE trade winds from the Sahara Desert (BNSG, 2017) [8]. The temperature of the area is typical of the entire middle belt region of Nigeria, it is at its lowest during the peak months of harmattan (January and December).

The vegetation of Makurdi is the Guinea savannah with trees and tall grasses mixed together having average height. The natural vegetation consists of woodland and tall grass. The guinea savannah has isolated forests, patches of woodland, scrubs and shrubs in addition to tall grasses (Abah, 2014) [1]. Halima and Edoja, (2016) [15] and Hula, (2014) [19] observed that the vegetation of the area was hitherto covered by forest but due to uncontrolled and continuous clearing of the vegetation for agricultural activities together with other anthropogenic activities such as burning of the bushes, grazing and hunting among others, have to a large extent, impacted on the original forests. The original forest vegetation is now reduced to secondary forest and savannah vegetation. The appearance of the vegetation cover of the area varies according to the season. During rainy season, the vegetation becomes very fresh and greenish but wither and die away in the dry season. Some trees are deciduous shading their leaves during the dry season but regain their leaves with the onset of the next rainy season. The plants have adaptive features to enable them overcome the drought conditions by developing long taproots, leathery leaves and succulent stems (Hula, 2014) [19]

Continuous clearance of the forest vegetation has given rise to the emergence of secondary vegetation at various stages of growth. The grasses grow very tall and are coarse when matured. There are pockets of scattered trees that are of economic benefits and they include mango, shea butter, locust bean, African iron, Isoberlinia, cashew, *Danielliaoliveri*, *Gmelina arborea*, oil palm, etc. These trees produce products that serve as raw material for some small-scale industries.

The drainage system of the area is influenced by factors such as relief, climate, rock structure and human activities in the area. The major drainage feature in the area is the River Benue which is the major tributary of the River Niger. It takes its source from the Cameroonian Mountains, and flows through central Nigeria, and meets the River Niger at Lokoja in Kogi State about 483000m from the coast. During the rainy season between May and September, the river is navigable and is used for transportation purposes, as well as for tourism, fishing and irrigated farming (BNSG, 2017) [8]. Two major rivers in Makurdi are River Benue and River Katsina-Ala, and they have many smaller tributaries such as Mu, Guma. Several other rivers and streams do not empty their waters into these two major rivers. These rivers and streams provide extensive alluvial floodplains that are utilised extensively for irrigation farming.

2.2 Methodology: Data Requirement and Collection

The data used for this research came from primary and secondary sources. The primary data involved personal observation, taking of pictures; and taking of locational points using handheld Global Positioning System (GPS). The GPS was also used for ground truthing during image classification. The secondary data used consists of Satellite Remote Sensing imageries, Digital Elevation Model (DEM), Population data, Road network, Rail network and drainage network.

Satellite imageries used included Landsat TM (1987); Landsat ETM+ (2007); and Operational Land Imager (OLI) (2017). The Landsat imagery dataset was sourced from the *Earthexplorer* platform from United States Geological Surveys (USGS), Global Land Cover Facility (GLCF) and GloVis. Changes in land cover were measured using time series of remotely sensed data (Landsat TM, ETM and OLI). Table 1 gives a summary of the image characteristics for the dataset used. Dry season images of the three data sets were acquired from January to March in order to reduce the effects of clouds that are prevalent during the rainy season. Because the images are from the same season and comparable climatic conditions, it enhanced the classification as the spectral reflection of most features are easily comparable across the different images. In addition, high resolution Google earth images were used to aid in classification.

Table 1: Specifications of Satellite Imageries Used

Satellite	Path/Row	Sensor	No of Bands	Bands used	Date Acquired	Spatial Resolution
Landsat	188/54,55 187/55,56	TM	7	NIR, R, G (4,3,2)	29/01/1987	30m
Landsat	188/54,55 187/55,56	ETM+	8	NIR, R, G (4,3,2)	21/12/2007	30m
Landsat	188/54,55 187/55,56	OLI	11	NIR, R, G (5,4,3)	16/02/2017	30m
ASTER GDEM*	-	Radiometer	1	-	2011	30m

TM= Thematic Mapper, ETM+= Enhanced Thematic Mapper Plus, OLI = Operational Land Imager:

***Source*:** Modified from (Northrop, 2015)* http://www.gisat.ez/content/en/products /digital-elevation-model/aster-gdem

The Digital Elevation Model (DEM) data used were the Advanced Spaceborne Thermal Emission and Reflection Radiometer (ASTER) DEM, (Table 1). The data is a raster data format, having spatial resolution of 30 meters and a scene coverage of 1º x 1º (approximately 111 km x 111 km). The data were downloaded using the *Earthexplorer* online platform from United States Geological Surveys (USGS).A subset of the area covering the study area was done. The DEM was used for the determination of slope and elevations of points which affect the cost of construction. Higher slopes and marshy areas attract higher cost of construction as opposed to plain and gentle slopes.

Other ancillary data used include Population data from the National Population Commission, Transportation network from Google, and drainage network characteristics from Google Earth. The tools used for carrying out the research were; ArcGIS 10.2 used for pre-processing of images and vector data, ERDAS Imagine 2014, used for image processing, Idrisi Selva, used for classification, change detection and modelling, Google Earth Image, used for delineation and updating of transportation and drainage maps, Global Positioning System, used for classification and data validation

2.3 Image pre-processing

In order to map the types and extent of LULC classes in Makurdi, the data were subjected to some processing and analytical procedures. Landsat TM, ETM and OLI were pre-processed, so that inherent errors and formatting that are required for further direct processing of the data were taken care of. The downloaded Landsat images were in separate bands and need to be layer stacked. This is a process whereby different bands of an image are combined together to form a single multispectral image. These individual bands were then stacked sequentially from 1 to 7 using ERDAS Imagine 2014. When layer stacking of all the bands from each scene was completed, the produced multispectral image from the scenes was then mosaicked. Specifically, the three (3) satellite imageries, Landsat TM (1987); Landsat ETM+ (2007); and Landsat OLI (2017) were corrected radiometrically through haze removal operations, so that radiometric errors added to data, due to atmospheric scattering were corrected, using the ERDAS Imagine 2014 image processing software. Radiometric correction refers to the elimination of distortions in the degree of electromagnetic energy registered by each detector. Focal analysis module in ERDAS 2014 was used in removing scan lines on images especially the 2007 Landsat image. Geometric correction refers to the process of co-registration of the satellite images, so that the images could overlap in the best possible way. This function was achieved in IDRISI through the RESAMPLE module. This is very essential due to the fact that some of the essential methods are based on the comparison of the two images from different time periods, e.g. supervised classification although most of Landsat images have been already georeferenced, images with a lot of cloud cover could have low geometric accuracy, and therefore required to be geo-referenced.

In order to obtain images that are cloud free, mosaicking of two or more images of the same area was performed in order to replace pixels affected by clouds with cloud free pixels from another image. In order to do this, accurate geometric registration among images was done. For radiometric compatibility, it is imperative that mosaic is done between images of the same season. In effect, the appearance of vegetation varies greatly during the year; therefore, all the images need to be acquired in less than one month, or at least be acquired exactly in the same month of different years (Congedo and Munafò, 2012) [10]. The area of study covers more than a single scene of Landsat. As a result, several scenes were acquired as shown in Table 1. The Digital Elevation Model (DEM) data were used to produce elevation and slope characteristics of the area.

The images were cut to the desired shape through clipping of the study area using the already mosaicked scenes. The shapefile of Makurdi was used to clip from the larger scenes that were earlier mosaicked. The technique used was the subset method in ERDAS 2014 and the desired shapefile of Makurdi was used as the Area of Interest (AOI). The choice of this method was based on its simplicity of use and its higher accuracy. This is because the mosaicked area is larger than the Area of interest (AOI) and it helps in defining precisely the study area.

Image enhancement increases the contrast among different features thereby enhancing easy identification of features and subsequent classification. After the enhancement process, band combination operations were performed to select the different bands which will enable the classification of a given earth surface feature. The major reason for colour composite is to highlight certain brightness values that are associated with certain surface features. A band combination of 4, 3, 2 (for RGB) was used for the Landsat TM and ETM images and 5, 4, 3 for OLI images as this produced superior results. It is suitable for urban application and delineating land, water and vegetation boundaries.

2.4 Image classification

A per-pixel image classification method for ground cover analysis was used through a supervised classification algorithm which is a procedure for categorizing spectrally similar areas on an image by identifying "training" sites of known targets and then generalizing those spectral signatures to other areas of targets that are unknown *(*Mather and Koch, 2011). It is a process of using samples whose identity is known to categorize samples whose identity is unknown. A Maximum Likelihood algorithm of supervised classification was adopted because of the author's familiarity with the terrain. This method was chosen because it is easier to accomplish and more so, the large volume of images to be interpreted could not warrant the use of visual on-screen interpretations. The visual method depends largely on the skill and familiarity of the interpreter and is therefore prone to much error if the interpreter is not well experienced. The identification of training sites used was based on spontaneous recognition and logical inference both of which are products of visual interpretation. Spontaneous recognition refers to the capability of the interpreter to recognize objects at a glance such as agricultural plots. In logical inference, the interpreter draws conclusion on the basis of ground control points, his professional knowledge and field experience over the years (Congedo and Munafò, 2012) [10]. The Maximum Likelihood is one of the most commonly used supervised classifiers, which uses the Gaussian threshold stored in each class signature to assign every pixel a class (Huang *et al*., 2009) [18]. Maximum Likelihood classification assumes that the probability distributions for the classes follow the normal distribution model (Richards and Jia, 2006) [31]. The discriminant function, as described by Richards and Jia, (2006) [31], is:

$$g_i(x)=\ln p(\omega_i)-\tfrac{1}{2}\ln|\Sigma_i|-\tfrac{1}{2}(x-m_i)^t \Sigma_i^{-1} (x - m_i) \quad (1)$$

Where: ω_i = class (where i = 1, M and M is the total number of classes)

x = pixel vector in n-dimension where n is the number of bands

p (ω_i) = probability that the correct class is ω_i occurs in the image and is assumed the same for all classes

$|\Sigma_i|$ = determinant of the covariance matrix of the data in class ω_i

Σ_i^{-1} = inverse of the covariance matrix and m_i = mean vector

The Maximum Likelihood method was used, because it is one of the best classification methods which assigns pixels to the class with the largest probability to determine class membership of a

particular pixel. In choosing training sites, colour composite images formed by the combination of three individual monochrome images, which highlight certain surfaces, and help photo-interpretation were viewed. Each band is assigned to a given colour: Red, Green and Blue (RGB) (NASA, 2011) [24]. A Supervised classification of Landsat image data for the three periods (1987, 2007 and 2017) was performed using the Maximum Likelihood Classifier to identify and map land use and land cover classes. The first stage involves the classification of Makurdi while in the second stage, four major cities in four Local Government Areas (Makurdi, Gboko, Otukpo and Katsina-Ala) were classified. In order to ascertain the areal extent and rate of change in the LULC of Makurdi, the following variables were computed.

Total area (T_a), Changed area (C_a), Change extent (C_e) and Annual rate of change (C_r) these variables can be described by the following formula as given by: Yesserie (2009)

$$C_a = T_a(t_2) - T_a(t_1); \quad (2)$$

$$C_e = C_a / T_a(t_1); \quad (3)$$

Where t_1 and t_2 are the beginning and ending times of the land use and land cover studies conducted.

Table 2: Classification scheme adopted.

S/N	Class	Description
1	River/ water bodies	Open water features including lakes, rivers, streams, ponds and reservoirs.
2	Built-up/Urban Areas	Urban and rural built-up including homestead area such as residential, commercial, industrial areas, villages, settlements, road network, pavements, and man-made structures.
3	Grassland	Areas dominated by grasses including vegetated sandbars and grazing areas/
4	Bare surface	Fallow land, earth and exposed river sand land in-fillings, construction sites, excavation sites, open space and bare soils.
5	Forest	Trees, natural vegetation, mixed forest, gardens, parks and playgrounds, grassland, vegetated lands.
6	Farmlands	Areas consisting of cultivated lands used for the production of annual crops, perennial woody crops. Agricultural lands, and crop fields.

***Source*:** Modified from Anderson *et al*. (1976) [5]

Fieldwork was done so as to collect geographical data to map land cover and for accuracy assessment of the land cover classification. Ground-truth data were also collected on spatial features from the study area, such as spatial location, land cover and land use, road network with the aid of a GPS. Ground truthing enabled the collection of inference data and to increase ones' knowledge of land cover conditions. It also enables familiarity of features as they appear on the satellite image on the computer screen, for verification and validation of the interpreted results. The process of identifying and transferring ground points onto the screen was done using the GPS. Each LULC class was physically identified in the field and the position of the area recorded using GPS which was later transferred to the image whereby it was easier to identify the appearance of such land uses and land cover on the screen. Inaccessible areas were complimented with the use of Google earth images. In summary, both visual interpretation and digital image classification methods were employed in data interpretation.

2.5 Accuracy Assessment

The accuracy of satellite image classification could be inhibited by the resolution of images used and dearth of fine details as well as unavoidable generalization impact and therefore, errors are always expected. This is why, to ensure wise utilization of the produced LULC maps and their associated statistical results, the errors and accuracy of the analysed outputs should be quantitatively explained (Siddhartho, 2013) [34]. Accuracy assessment is a process whereby the final product of classification is compared with ground truth or reliable sources so as to assess the extent of agreement or disagreement. This study adopted the Error Matrix approach as used by Friehat *et al*, (2015) to assess the accuracy of the classification.

Accuracy assessments of the classified maps (1987, 2007 and 2017) were done using the error matrix (ERRMAT in Idrisi Selva). The error matrix assesses accuracy using four parameters which include overall accuracy, user's accuracy, producer's accuracy and the Kappa Index of agreement (KIA). The overall accuracy specifies the total pixels correctly classified and is derived by dividing the total number of pixels correctly classified by the total number of pixels in the error matrix. The producer's accuracy defines the probability of a reference pixel being correctly classified. It represents the error of omission. The number of samples correctly classified for a given column is divided by the total for that column (Pedro, 2015). The user's accuracy on the other hand defines the probability that a pixel classified on a map actually represents that category on the ground. User's accuracy represents the error of commission. This can be calculated by dividing the number of samples correctly classified for a given row by the total of the row (Pedro, 2015). On the other, the Kappa index measures the agreement between classification map and reference data (Congalton and Green, 2008). All accuracy parameters have index values between 0 and 1, where 0 symbolizes poor and 1, strong classification accuracy/agreement.

The Kappa statistics formula developed by Cohen Kappa in 1960 and modified by Jenness and Wynne (2007) was adopted for calculating Kappa statistic. It has the advantage of correcting for chance agreements between the observed and predicted values.

$$k = \frac{N\sum_{i=1}^{n} m_{i,i} - \sum_{i=1}^{n}(G_i C_i)}{N^2 - \sum_{i=1}^{n}(G_i C_i)} \quad (4)$$

Where: *i* is the class number

N is the total number of classified pixels that are being compared to ground truth

mi, i is the number of pixels belonging to the ground truth class i, that have also been classified with a class i (that is, values found along the diagonal of the confusion matrix)

Ci is the total number of classified pixels belonging to class i

Gi is the total number of ground truth pixels belonging to i

Kappa value changes from -1 to +1 and the interpretation of the values can be determined according to these values:

< 0: Less than chance agreement

0.01–0.20: Slight agreement

0.21– 0.40: Fair agreement

0.41–0.60: Moderate agreement

0.61–0.80: Substantial agreement
0.81–0.99: Almost perfect agreement. (Borana and Yadav, 2017) [9].

Under ideal conditions, the accuracy of the classification ought to be assessed by overlaying an already existing LULC map. Due to absence of already existing LULC classification for Makurdi, handheld Garmin GPS receiver was used to take coordinates of selected LULC as ground control points from the field complimented with Google Earth images. The points of these reference data were determined through stratified random sampling by identifying and locating the land use classes of interest in the field and their GPS points and coordinates taken at ±3m accuracy and recorded as was used by Appiah (2016).

The methodology for analysing the trend of land use and land cover changes from 1987- 2017 was through the use of Change Analysis Tab in IDRISI. Here, the focus was on the spatial trend of change panel to directly detect the actual spatial pattern of each major land conversion that has taken place in Makurdi from 1987-2007, 2007-2017 and1987-2017. The principle under which this panel works is the polynomial order in which the spatial pattern and trend of land use and land cover between two periods is generalized. According to Eastman (2012) [12], the spatial trend of change panel in LCM is to follow a similar pattern on Trend Surface Analysis (TSA) as in the TREND module in IDRISI. It calculates trend surface polynomial equations up to the 9th order for spatial data sets, and then interpolates the surfaces based on those equations. The generic equation for the polynomials fitted by TREND as given by (Saifullah, Barus, & Rustiadi, 2017) [33] is:

$$Z = \sum_{i=0}^{k} \sum_{j=0}^{i} bij\, X^{i-j}\, y^{j} \quad (5)$$

Where k = is the maximum order to be fitted;
b = coefficient of the polynomial equation; both *i*and *j* are iteration variables associated with *k*, in which *i = 0, k* and *j = 0, i*. (Saifullah et al., 2017) [33]

After a successful classification, the LULC classes for 1987, 2007 and 2017 were compared to determine the extent of change. The extent of change was divided by the time interval between the initial and the later date to arrive at the rate of rural- urban conversion. This operation is represented by the following equation as given by Yesserie (2009):

$C_r = C_e / (t_2 - t_1)$; (6)

Where C_e = Change extent
t_1 and t_2 = the starting and ending times respectively of the LULC studies conducted

3 Results and Discussion

Extent of land use and land cover types in Makurdi

A closer look at the classified images of Makurdi (Figures.2, 3 and 4 and Table 3) reveals that urban area accounted for 3.44% (2871ha) in 1987 and increased to 10.9% (9102ha) in 2007.

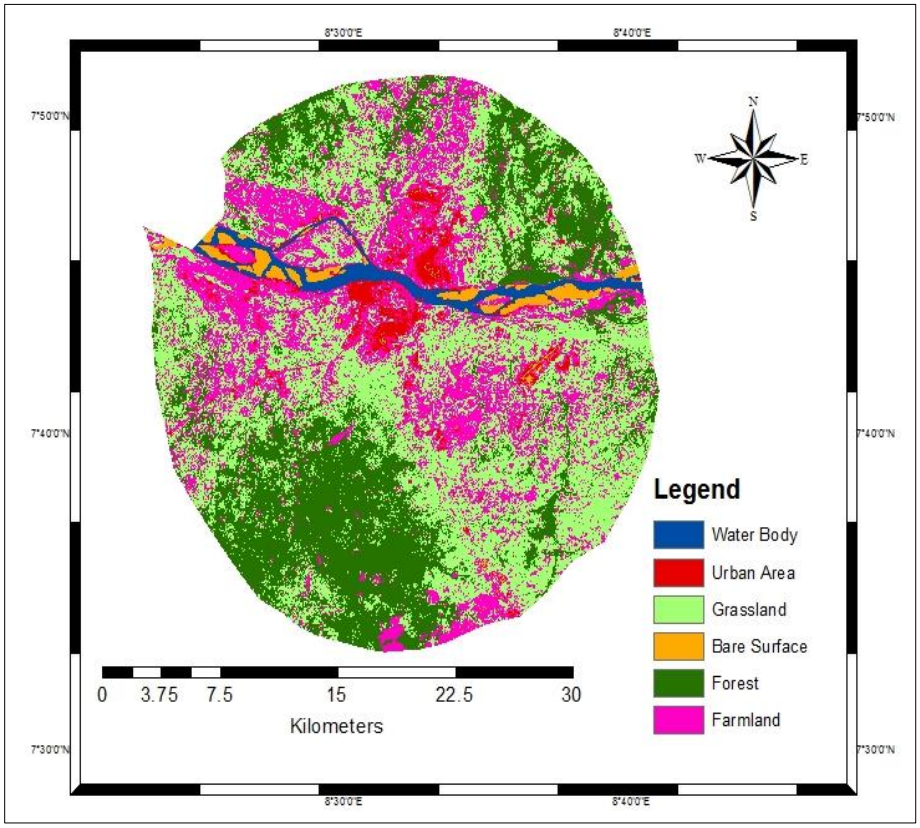

***Source*:** Author's fieldwork, 2018

Fig 2: Land use and Land cover map of Makurdi for 1987

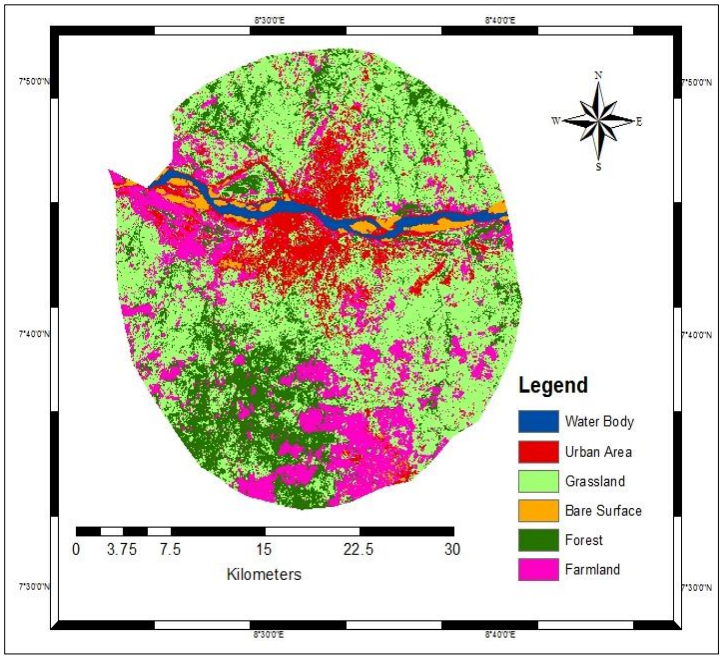

***Source*:** Author's fieldwork, 2018

Fig 3: Land use and Land cover map of Makurdi for 2007

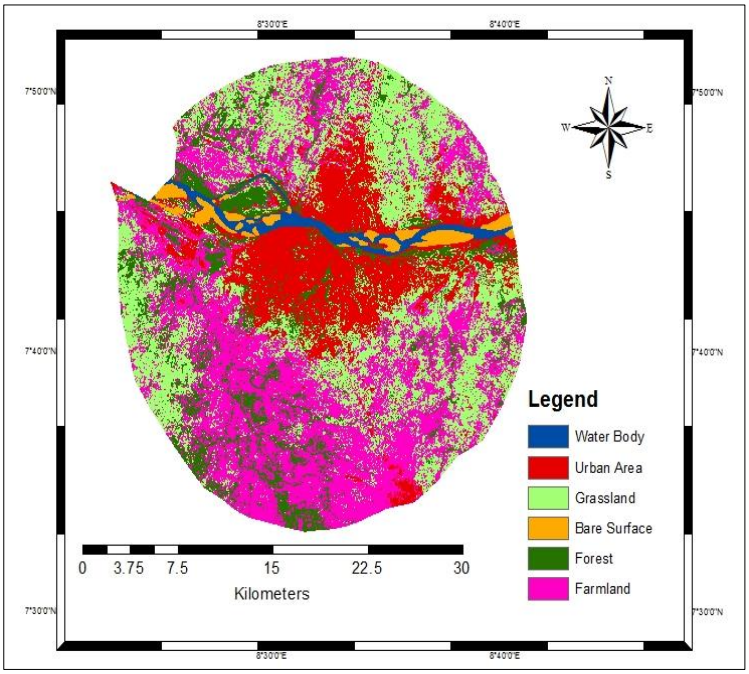

***Source*:** Author's fieldwork, 2018

Fig 4: Land use and Land cover map of Makurdi for 2017

It continued to expand in 2017 to 17.95% (14996ha). Although built up area has grown in all directions, the major areas of growth were the South-west, South and North-east of the area. Forest cover stood as the second largest cover type in 1987 being represented by 26.93% (22492ha). By 2007, the forest cover decreased to 18.55% (15494ha) and further decreased to 12.87% (1075ha) in 2017. The forest in the Southwest and Northeast have gradually given way to farming activities. Grassland which was the dominant land cover in 1987 accounted for 40.07% (33474ha) of the total area and increased to 46.99% (39250ha) by 2007. There was, however, a decline to 29.5% (24635ha) in 2017.The decline could be as a result of increase in farming activities during the period. Farmland covered 21062ha (25.22%) in 1987 and declined in 2007 to 15762ha (18.87%) but again rose to 29415ha (35.22%) in 2017. This fluctuation could be due to decline in prices of farm produce in 2007 and the rise in prices of same in 2017. Bare surface and Water body represent less than 3% for each of the three periods.

Table 3: Area Statistics of LULC in Makurdi (1987, 2007 and 2017)

Land cover Class	1987		2007		2017	
	Area (Ha)	Area (%)	Area (Ha)	Area (%)	Area (Ha)	Area (%)
Water Body	2046	2.45	1820	2.18	1817	2.18
Urban Area	2871	3.44	9102	10.9	14996	17.95
Grassland	33474	40.07	39250	46.99	24635	29.5
Bare Surface	1576	1.89	2093	2.51	1908	2.28
Forest	22492	26.93	15494	18.55	10750	12.87
Farmland	21062	25.22	15762	18.87	29415	35.22
Total Area	83521	100	83521	100	83521	100

***Source*:** Author's fieldwork, 2018

The accuracy of classification for the three periods of 1987, 2007 and 2017 for Makurdi showed an overall accuracy of 88.78%, 82.7% and 80.52% respectively (See Table 4). This was considered a decent overall accuracy and, therefore acceptable for the succeeding analysis and change detection. The user's accuracy for different classes ranged between 60.38% and 100% and the producer's accuracy ranged between76 % and97.14%. The overall Kappa index was also calculated for each classified map to determine the accuracy of the results. The results of the three periods 1987, 2007 and 2017 revealed Kappa statistics of 0.86, 0.79 and 0.76 respectively. The Kappa coefficient for the three periods ranges from substantial agreement to almost perfect agreement on the Kappa scale, an indication that it can be used

Table 4: Accuracy assessment result of LULC classification in Makurdi

LULC Class	1987 classification		2007 classification		2017 classification	
	Producer's Accuracy (%)	User's Accuracy (%)	Producer's Accuracy (%)	User's Accuracy (%)	Producer's Accuracy (%)	User's Accuracy (%)
Water Body	95	100	5.71	78.26	80.95	94.44
Urban Area	97.14	100	86.11	96.87	88.24	85.71
Grassland	83.78	83.78	85	70.83	82.05	60.38
Bare Surface	83.33	78.95	79.17	79.17	85.71	85.71
Forest	80.56	85.29	83.87	78.79	76	97.44
Farmland	91.53	87.1	75.76	100	77.27	78.46
Overall Accuracy	88.78%		82.7%		80.52%	
Overall Kappa	0.86		0.79		0.76	

***Source*:** Author's fieldwork, 2018

3.1 Trend and rate of change in LULC in Makurdi (1987, 2007 and 2017)

The trend in the land use and land cover changes in Makurdi from the first period (1987-2007) reveals that urban area increased by 6231ha (24.88%) where the annual rate of change was 4.98%. In the second period (2007-2017), urban areas increased by 5894ha (15.08%) with an annual rate of change of 1.51% (see Figure 8). The overall trend (1987-2017) showed that urban areas increased by12125ha (422.33%) with an annual rate of change of 14.07% (see Table 4.12). The continuous increase in urban area may probably be due the influx of population to the state capital in search of white-collar jobs. The establishment of Joseph Sarwuan Tarka University and Makurdi University in the city has also attracted a lot of student population. Forest land has diminished by 6998ha (31.11%) with the annual rate of change of -1.56% between 1987 and 200

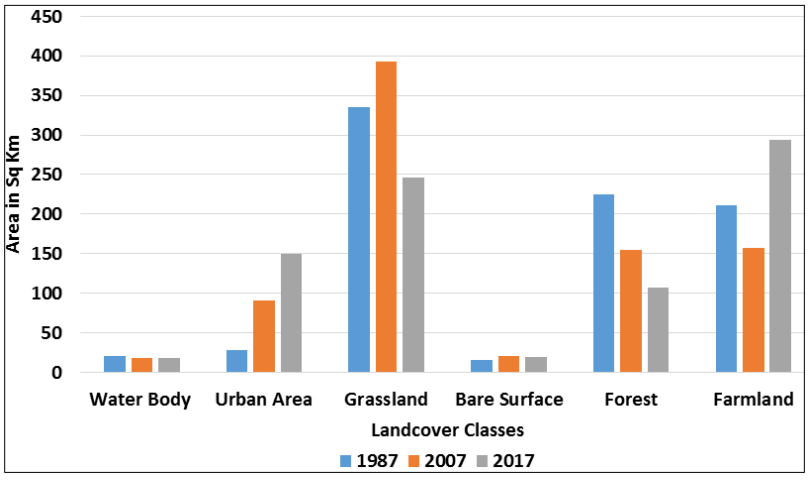

***Source*:** Author's fieldwork, 2018

Fig 5: Trend of Land cover changes in Makurdi (1987-2017)

Between 2007 and 2017, 4744ha (-30.62%) of forest was lost at an annual rate of 3.06%.

The overall trend showed that 11742ha (-52.21%) of forest was lost at an annual rate of 1.74%.

Table 5: Annual Rate of change for Makurdi (1987, 2007 and 2017)

LULC Class	1987-2007 Area(ha) Change	Percentage of Change	2007-2017 Area (ha) Change	Percentage of Change	1987-2017 Area (ha) Change	Percentage of Change	Annual Rate of Change		
							1987-2007 (%)	2007-2017 (%)	1987-2017 (%)
Water Body	-226	-11.05	-3	-0.16	-229	-11.19	-0.55	-0.02	-0.37
Urban Area	6231	217.03	5894	64.75	12125	422.33	10.85	6.48	14.07
Grassland	5776	17.26	-14615	-37.23	-8839	-26.41	0.86	-3.72	-0.88
Bare Surface	517	32.81	-185	-8.83	332	21.07	1.64	-0.88	0.7
Forest	-6998	-31.11	-4744	-30.62	-11742	-52.21	-1.56	-3.06	-1.74
Farmland	-5300	-25.16	13653	86.62	8353	39.66	-1.26	8.66	1.32

***Source*:** Author's fieldwork, 2018

This high rate of forest loss is very worrisome considering the dangers posed by deforestation. Grassland appreciated by 5776ha (17.26%) with an annual rate of change of 0.86% in the first period. By the second period, however, there was a sharp decline in the area of grassland by -14615ha (37.23%) at an annual rate of-3.72%. The decline was also noticed in the overall trend depreciating by 8839ha (26.41%) at an annual rate of -0.88%. Farmland witnessed a decrease in the first period declining by 5300ha (25.16%) but rising sharply in the second period by13653ha (86.62%) at an annual rate of 8.66%. The fluctuation in the pattern of change may be due to a reluctance to engage in farming at the initial time but a sudden change in attitude owing to government desire to enhance food security. Figure 4.8 depicts the trend in land use and land cover changes in Makurdi during the period.

Land change analysis using Land Change Modeler (LCM)

Makurdi, the state capital, witnessed a distinct land cover transition during the period. In the first period, grassland experienced the highest transition losing over 100ha but gaining over 150ha. Farmland and forest had more negative changes than positive changes resulting in the loss of these land cover classes. As can be seen from Figure (4.26a) urban area and bare surface increased. Farmland was the largest contributor to urban area expansion followed by grassland, forest and bare surface. This implies that the urban area is expanding at the expense of these land covers. The decrease in forest land was as a result of expansion in grassland and farmland. Areas hitherto occupied by forest have now been cleared and taken over by farms or abandoned as grassland. The second period (Figure 4.26b) showed a similar pattern. The transition among the land cover classes as grassland experienced the highest change followed by farmland, forest and urban area

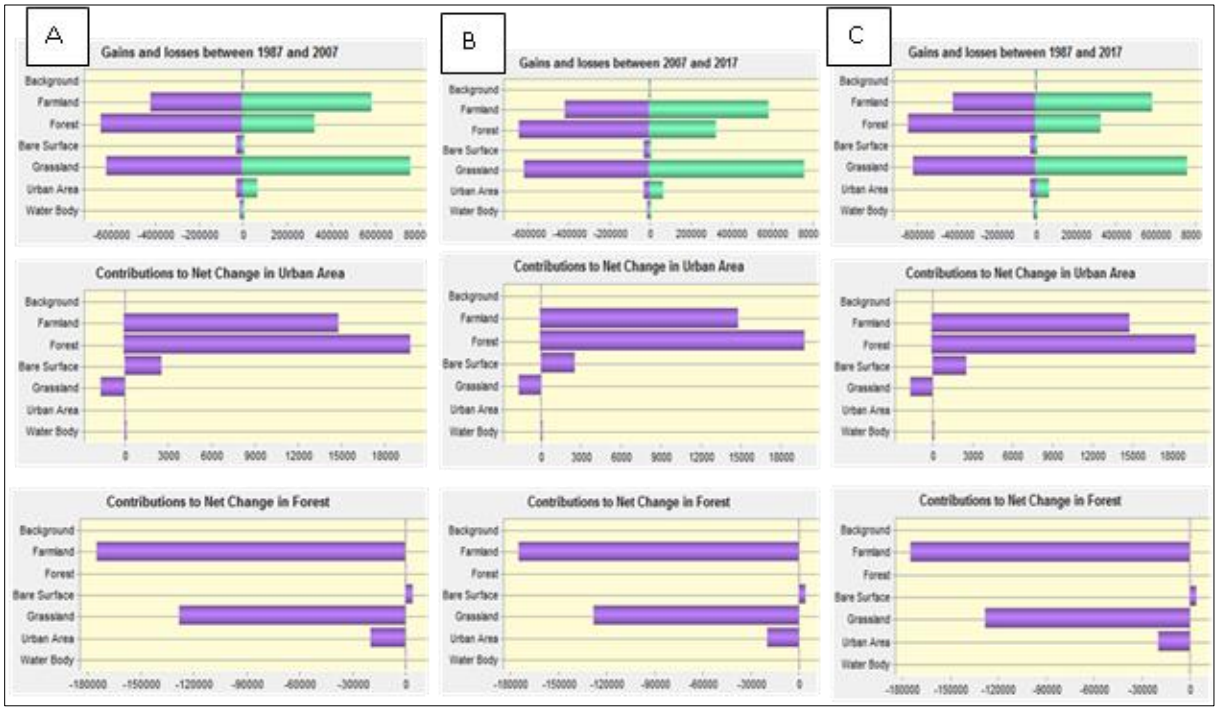

***Source*:** Author's fieldwork, 2018

Fig 6: Gains/losses of LULC classes, contribution to net change in Urban area and Forest (km^2) in Makurdi from (a):1987 – 2007, (b): 2007 -2017 and (c): 1987- 2017.

Drivers and their contribution to urban growth

In order to test the potential power of the drivers (explanatory variables), the LCM's Test and election of site and driver variable module was used. These set of explanatory variables were chosen based on preliminary investigations as well as reviews from relevant academic literatures. Table 4.19 shows the Cramer's V coefficient for each of the explanatory variables, As can be seen from the table, all the variables namely, likelihood of transition, distance from urban areas, roads, rivers, railways, digital elevation model (DEM), slope and population density selected for transition development were greater than 0.15, some of them were higher than 0.4 which indicates the selected variables have association with the changes and were used in the process as was shown by Wang and Maduako (2018). It is also evident that likelihood of transition, DEM and population density have values higher that 0.4, meaning that these three variables are strongly associated with transition and therefore kept in the sub-model structure. Also, the LCM MLP model results shown in Appendices B to F reveal that likelihood of transition, distance from urban areas and railways were most important drivers in shaping urban growth as revealed by the influence order.

Table 6: Cramer's V Test values for explanatory variables

Variable	Cramer's V Value
Likelihood	0.4261
Dist_Urban	0.3756
Dist_Roads	0.3200
Dist_Rivers	0.3375
DEM	0.4274
Slope	0.3964
Pop density	0.4252
Dist_Rails	0.1829

***Source*:** Author's fieldwork, 2018

4.8 Sensitivity Analysis

Upon completion of the entire process, MLP outputs a number of statistics that provide information regarding the power of the explanatory driver variables as well as the models accuracy in predicting class transitions and persistence. One important aspect of the statistics generated is termed "Forcing Independent Variables to be Constant". After the system has trained on all of the explanatory variables, the system tests for the relative power of explanatory variables by selectively holding the inputs from selected variables constant. Holding the input values for a selected variable constant effectively removes the variability associated with that variable. Using the modified model, the MLP procedure repeats the skill test using the validation data. The difference in skill thus provides information on the power of that variable. This process is repeated for all the driver variables to determine their influence on the skill measure and accuracy of the model.

Three different sensitivity analyses were run. In the first section, a single variable is held constant. This is repeated for all variables. Table 4.20 shows the sensitivity of holding one variable constant for each of the five selected areas. In the second sensitivity, all variables are held constant (at their mean values) except one.

Table 7: Forcing a Single Independent Variable to be Constant

Model	Independent Variables	ACC (%)	SM	IO
With all Variables		75.97	0.7117	N.A
Var. 1 constant	Distance from urban area in 1987	64.76	0.5772	2
Var. 2 constant	Distance from roads	75.36	0.7043	6
Var. 3 constant	Distance from rivers	75.07	0.7008	5
Var. 4 constant	Digital elevation model	74.04	0.6884	4
Var. 5 constant	Slope	76.03	0.7123	7
Var. 6 constant	Population density	76.18	0.7142	8*
Var. 7 constant	Evidence likelihood of transition	25.28	0.1034	1**
Var. 8 constant	Distance from railways	73.34	0.6800	3

***Source*:** Author's fieldwork, 2018

Key: Acc= Accuracy, SM= Skill measure, IO= Influence order, ** = Most Influential, * = Least Influential

The final test in section 3 is entitled Backwards Stepwise Constant Forcing. Starting with the model developed with all variables, it then holds constant every variable in turn to determine which one has the least effect on model skill. Step 1 thus shows the skill after holding constant the variable that has the lowest negative effect on the skill. If a variable is held constant and the skill does not decrease much, then it suggests that that variable has little value and can be removed (See Table 8). It then tests every possible pair of variables that include that determined in step 1 to figure out which pair, when held constant, have the least effect on the skill. It continues in this manner progressively holding another variable constant until only one variable is left. The backward stepwise analysis is very useful for model development. The backward stepwise MLP result was used in assessing the best model combination of independent variables based on percentage accuracy and skill measure by

consecutively eliminating the weakest independent variable one by one.

The results of the backwards stepwise constant forcing in Table 8 shows that for Makurdi all the eight independent variable combination had an accuracy rate of 75.97% and 0.7117 of skill measure. MLP rerunning test with the elimination of variable 6 (population density) had a higher accuracy rate of 76.18% and a 0.7142 of skill measure compared to the use of all the eight variables. But the removal of variables 6 and 5 (population density and slope) yielded the highest accuracy of 76.27% and a 0.7152 of skill measure compared to 75.97% accuracy and 0.7119 of skill measure when all the variables were used.

Table 8: The Result of MLP with backwards stepwise constant forcing

With all variables	All variables	75.97	0.7117
Step 1: var.[6] constant	[1,2,3,4,5,7,8]	76.18	0.7142
Step 2: var.[6,5] constant	[1,2,3,4,7,8]	76.27	0.7152
Step 3: var.[6,5,2] constant	[1,3,4,7,8]	75.43	0.7052
Step 4: var.[6,5,2,3] constant	[1,4,7,8]	74.91	0.6989
Step 5: var.[6,5,2,3,4] constant	[1,7,8]	73.04	0.6765
Step 6: var.[6,5,2,3,4,8] constant	[1,7]	70.42	0.6450
Step 7: var.[6,5,2,3,4,8,1] constant	[7]	50.06	0.4007

***Source*:** Author's fieldwork, 2018

Transition Potential Modelling using MLP

After selecting the predictor variables, all the transitions were then modeled in one transition sub-model called urban area, as they had the same driving forces, with the aim of producing the transition maps. As earlier stated, MLP was used in modelling the transitions and it generated transition potential maps for each of the evaluated transition sub-models. The results of the MLP transition modelling is presented in Figures 7 which shows three transition maps that were created which include transition from grassland to urban area, forest to urban area and farmland to urban area. These transition potential maps generated from MLP modelling were then used in Markov Chain model for determining the amount of change to be expected for each transition and for predicting of future scenarios.

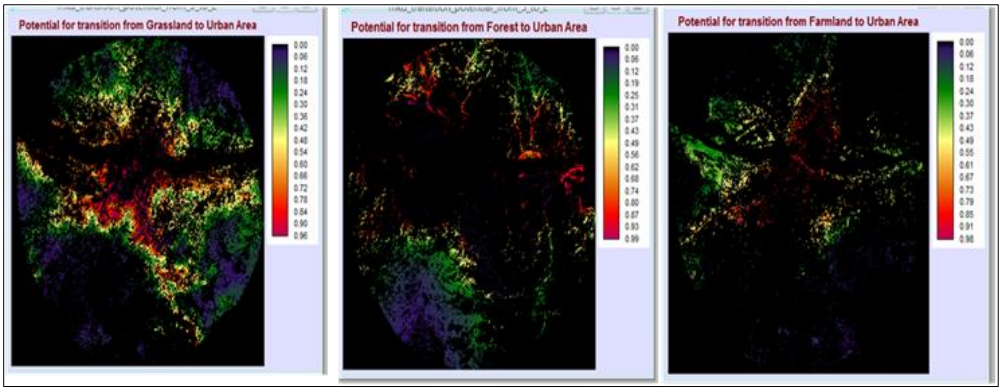

***Source*:** Author's fieldwork, 2018

Fig 7: Transition potential maps for Makurdi

Model Predictions and Validations

Figures 8 shows the classified and predicted land cover maps of Makurdi for the year 2017. It is noticeable from it that the model under-predicted urban area extent while it over-predicted grassland.

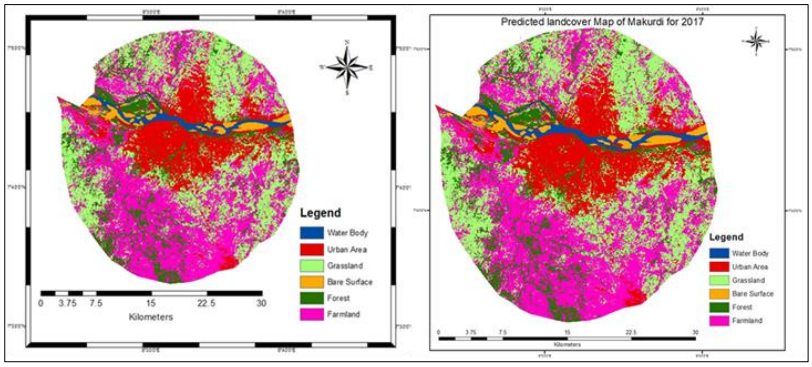

***Source*:** Author's fieldwork, 2018

Fig 8: Land cover maps of Makurdi for 2017 (Classified, left and predicted, right)

Table 10: Projected land cover statistics for 2030

Land cover	Benue		Makurdi		Gboko		Otukpo		Katsina-Ala	
	Area (Ha)	Area (%)	Area (Ha)	Area (%)	Area (Ha)	Area (%)	Area (Ha)	Area (%)	Area (Ha)	Area (%)
Water Body	21106	0.67	1820	2.18	217	0.11	3409	2.55	3247	1.21
Urban Area	122436	3.91	17384	20.81	18157	9.46	16819	12.60	17083	6.35
Grass land	1627370	51.99	41689	49.91	104756	54.55	65986	49.43	115669	43.02
Bare Surface	13964	0.45	1781	2.13	8217	4.28	6830	5.12	605	0.23
Forest	523009	16.70	8557	10.25	14277	7.43	14660	10.98	25431	9.46
Farm land	822515	26.28	12290	14.72	46424	24.17	25787	19.32	106829	39.73
Total	3130386400	100	83521	100	192048	100	133491	100	268864	100

***Source*:** Author's fieldwork, 2018

The results of the year 2030 prediction for Makurdi shows that grassland will be the dominant class as it will increase by 20.41% to 49.91% from 29.5% between 2017 and 2030 (see Table 4.25 and Figure 4.42). Urban area is estimated to increase by 2.86% to 20.81% from 17.95% between the periods under reference to become the second largest class after grassland. It is predicted to extend to the North West and south eastern parts of Makurdi. In contrast, farmland. Forest and bare surfaces are estimated to decline by 20.5%, 2.6% and 0.15%respectively yielding 12290ha, 8557ha and 1781ha (14.72%, 10.25% and 2.13%) respectively. The decline in area of the predicted farmland is similar to the results obtained by Attaallah (2018), who predicted that agricultural land in the Gaza Strip will decline by 5.6% by 2036 to the advantage of urban areas. Similar results were obtained by Ozturk (2015) [28]; Raziq, *et al*, (2016); Rimal, *et al*, (2017); Padmanaban *et al*., (2017). This result, however, is at variance with that predicted by Ansari and Golabi (2019) in which agricultural area was estimated to grow by 4.17% between 2015 and 2030 in Meighan Wetland, Iran. The variation can be explained by the fact that Meighan is an agricultural area while Makurdi is an urban area.

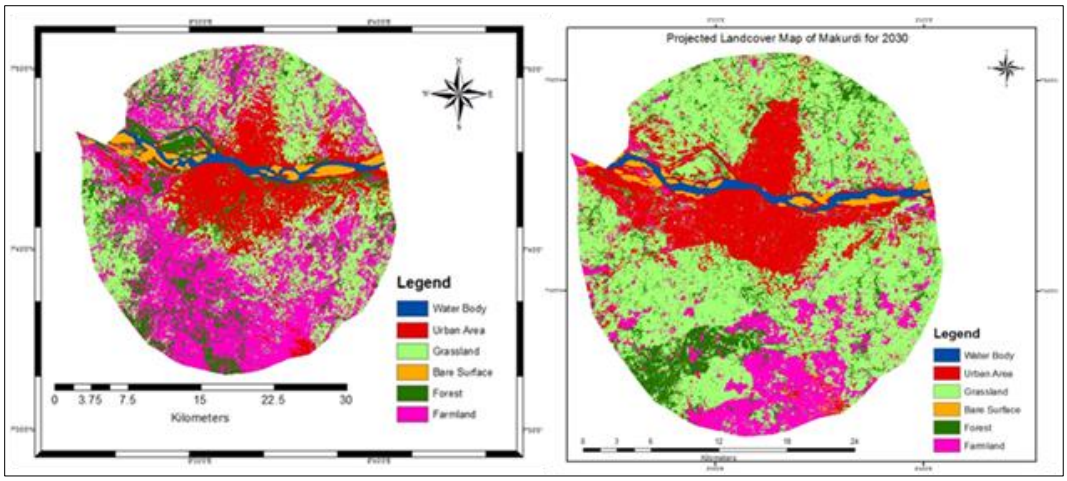

***Source*:** Author's fieldwork, 2018

Fig 9: Land cover maps of Makurdi (2017 left, and 2030 projected, right)

Table 11: Changed areas between LULC in 2017 and LULC in 2030 for Makurdi

Land cover Classes	LULC in 2017		LULC in 2030		Change	
	Area (Ha)	Area (%)	Area (Ha)	Area (%)	Area (Ha)	Rate %
Water Body	1817	2.18	1820	2.18	3	0
Urban Area	14996	17.95	17384	20.81	2388	+2.86
Grassland	24635	29.5	41689	49.91	17054	+20.41
Bare Surface	1908	2.28	1781	2.13	-127	-0.15
Forest	10750	12.85	8557	10.25	-2193	-2.6
Farmland	29415	35.22	12290	14.72	-17125	-20.5
Total	83521	100	83521	100		

***Source*:** Author's fieldwork, 2018

The result of the 2030 projection for Gboko shows that farmland, urban area and bare surface will increase by 10.52%, 0.81% and 2.98% respectively between 2017 and 2030 to occupy 46424ha (24.17%), 18157ha (9.46%) and 8217ha (4.28%) respectively as shown in Table 4.26 and Figure 4.43. Grassland, forest and water body are estimated to decline by -12.99%, -1.28% and -0.04% respectively. The expansion of the urban area is due to increase in rural-urban migration of youth in search of good jobs and the increasing desire to enjoy social and infrastructural amenities in the urban centre.

Soft Prediction

The soft prediction output is made up of maps that show the probability of change for a given set of transitions. The result of the soft prediction for 2030 is presented in figure 10. The soft output represents a continuous mapping of vulnerability to change for selected set of transitions. This prediction identified the extent to which the land area has the vulnerability to be changed. The soft prediction output detected the areas with

varying degrees of vulnerability instead of identifying what and how much of land cover categories would be changed. From the modelled output, it is evident that the North West and south west have higher degree of vulnerability than the other areas with this set of driving variables and identified individual transitions from one type to another.

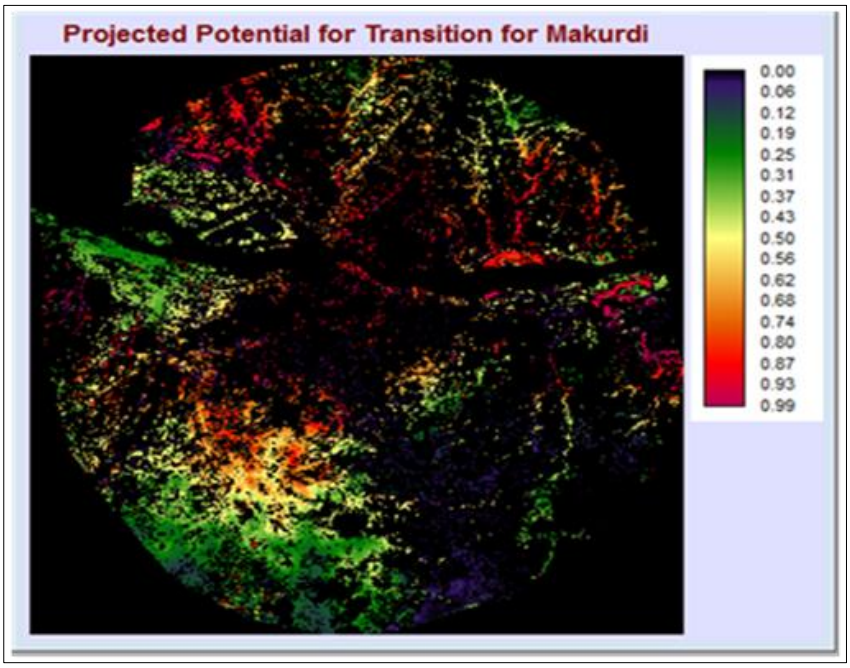

Fig 10: Map of soft prediction

Impact of Urban Growth on Deforestation

The situation in Makurdi reveals that urban area is ranked third in contributing to deforestation taking up 422ha of land during the period. Farmland and grassland were the largest contributors to urban expansion in the area as can be seen in Figure 11.

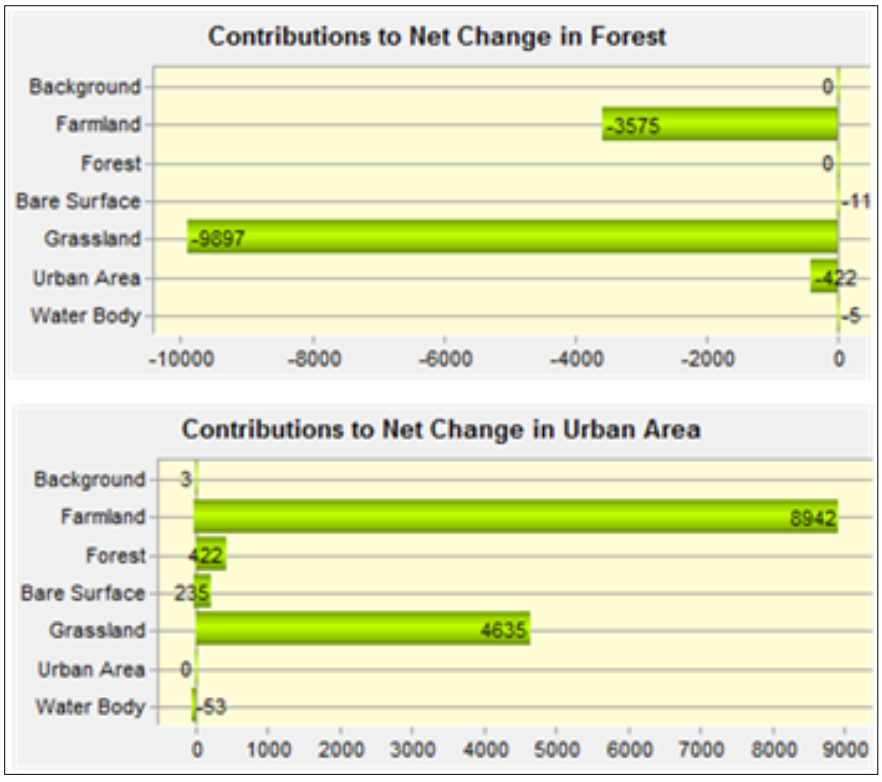

***Source*:** Author's fieldwork, 2018

Fig 11: Contributions to net change in forest and urban area from 1987-2030 in Makurdi

Conclusion

Urban growth has continued to be a threat to the existence of forest for a long time due to deforestation. The depleting forest resources is a threat to biodiversity as rightly stressed by Ohwo and Abotutu (2015). The results indicated that urban growth is one of the major drivers of deforestation in Makurdi. This results agree with that of Zhou, *et al*, (2017) where the effect of urban expansion of six mega-regions of China on forest loss was examined. Deforestation due to urban expansion leads to habitat alteration which results in the endangering and extinction of species accompanied by long lasting habitat loss. Apart from reducing the richness of native species, urbanization increases the dominance of nonnative species in the area (Kharel, 2010). These constitute serious challenge to environmental sustainability. The various species of plants and animals that are required to establish and sustain the various food webs and chains as well as natural cycles are systematically being depleted and thus resulting in ecological imbalance and threatening the survival of man in the environment as observed by Ohwo and Abotutu (2015).

Agricultural expansion is also affected by urban expansion as areas previously under cultivation are converted to urban areas. This has the effect of reducing areas under cultivation especially at the fringes where there exist barriers to prevent further expansion of these agricultural areas. This has a tendency of reducing farm output if intensive practices are not adopted. Where there are no barriers, there is the tendency for cultivated areas to expand further to accommodate the loss to urban areas thereby causing more deforestation.

References

1. Abah RC. Rural perception to the effects of climate change in Otukpo, Nigeria. Journal of Agriculture and Environment for International Development. 2014; 108(2):153-166. https://doi. org/10.12895/jaeid.20142.217
2. Ade M. Application of Geographic Information Systems in Land Suitability Rating for Lowland Rice Production in Makurdi. Ethiopian Journal of Environmental Studies & Management. 2014; 7:695-708.
3. Ahmed B, Ahmed R, Zhu X. Evaluation of Model Validation Techniques in Land Cover Dynamics. ISPRS International Journal of Geo-Information. 2013; (2):577-597. https: //doi.org/10.3390/ijgi2030577
4. Al-shalabi M, Billa L, Pradhan B, Shattri Mansor, Al-Sharif AA. Modelling urban growth evolution and land-use changes using GIS based cellular automata and SLEUTH models: the case of Sana' a metropolitan city, Yemen. Environmental Earth Sciences. 2012; 70(1):425-437. https://doi.org/10.1007/s12665-012-2137-6
5. Anderson JR, Hardy EE, Roach JT, Witmer RE. A Land Use and Land Cover Classification System for Use with Remote Sensor Data (Fourth). Washington: United States Department of the Interior, 1976.
6. Ansari A, Golabi MH. Prediction of spatial land use changes based on LCM in a GIS environment for Desert Wetlands – A case study : Meighan Wetland, Iran. International Soil and Water Conservation Research. 2019; 7(1):64-70. https://doi.org/10.1016/j.iswcr.2018.10.001
7. Attaallah H. Modeling of built-up lands expansion in Gaza Strip, Palestine using Landsat data and CA- Markov model. IOP Conf. Series: Earth and Environmental Science. 2018; 169:1-10. https://doi.org/doi :10.1088/1755-1315/169/1/ 01 2035
8. BNSG. In the Spotlight: Historical Background, 2017. Retrieved October 24, 2017, from https://benuestate.gov.ng/historical-background
9. Borana SL, Yadav SK. Prediction of Land Cover Changes of Jodhpur City Using Cellular Automata Markov Modelling Techniques. International Journal of Engineering Science and Computing. 2017; 7(11):15402-15406.
10. Congedo L, Munafò M. Development of a Methodology for Land Cover Classification in Dar es Salaam using Landsat Imagery. Rome, 2012.
11. Danburi CN. The Effect of Urban Encroachment on Guga Forest Reserve in Giwa Local Government Area, Kaduna State, Nigeria. Unpublished Master Thesis Ahmadu Bello University, Zaria, 2015.
12. Eastman JR. IDRISI Selva Tutorial. Idrisi Production, Clark Labs-Clark University, 2012, Vol. 45.
13. Ebrahimipour A, Saadat M, Farshchin A. Prediction of Urban Growth through Cellular Automata-Markov Chain. Bulletin de La Société Royale Des Sciences de Liège. 2016; 85(1):824-839.
14. Eltom IM, Elfaig AHI, Salih AAM. Urban Development and Deforestation: Urban Development and Deforestation : Evidences from. International Journal of Scientific and Research Publications. 2013; 3(10):1-9.
15. Halima CI, Edoja MS. Exploring the relationship between farming practices and vegetation dynamics in Makurdi, Nigeria. African Journal of Geography and Regional Planning. 2016; 3(1):218-225. Retrieved from http://wsrjournals.org/journal/wjas
16. Hegazy IR, Kaloop MR. Monitoring urban growth and land use change detection with GIS and remote sensing techniques in Daqahlia governorate Egypt. International Journal of Sustainable Built Environment. 2015; 4(1):117-124. https://doi.org/10.1016/j.ijsbe.2015.02.005
17. Hemba S, Iortyom ET, Ropo OI, Dam PD. Analysis of the physical growth and expansion of Makurdi Town using remote sensing and GIS techniques. Imperial Journal of Interdisciplinary Research. 2017; 3(7):821-827.
18. Huang SL, Wang SH, Budd WW. Sprawl in Taipei's peri-urban zone: Responses to spatial planning and implications for adapting global environmental change. Landscape and Urban Planning. 2009; 90:20-32. https://doi.org/10.1016/j.landurbplan.2008.10.010
19. Hula MA. Population Dynamics and Vegetation Change in Makurdi, Nigeria. Journal of Environmental Issues and Agriculture in Developing Countries, 2014, 2(1). https://doi.org/ 10.13140/2.1.4805.1847
20. Hussaini MU. The Impact of Economic Activities on Deforestation in Bauchi State. (A Theoretical perspective). IOSR Journal of Humanities and Social Science. 2014; 19(3):14-18.
21. Kharel G. Impacts of Urbanization on Environmental Resources: A Land Use Planning Perspective. Unpublished Master Thesis University of Texas Arlington, 2010.
22. Mishra VN, Rai PK, Mohan K. Original scientific paper. 2014; 64(1):111-127. https://doi. org/10.2298/IJGI1401111M

23. Musa SI, Hashim M, Reba MN. Urban Growth Assessment and its Impact on Deforestation in Bauchi Metropolis, Nigeria Using Remote Sensing and GIS Techniques. Asian Research Publishing Network Journal of Engineering and Applied Sciences. 2017; 12(6):1907-1914.
24. NASA. Landsat 7 science data users handbook. National Aeronautics and Space Administration Landsat, 2011. Retrieved from http://glovis.usgs.gov
25. Northrop A. IDEAS – LANDSAT Products Description Document. Bedfordshire, 2015. Retrieved from http://www.gisat.cz/content/en/products/digital-elevation-model/aster-gdem
26. Ohwo O, Abotutu A. Environmental Impact of Urbanization in Nigeria. British Journal of Applied Science & Technology. 2015; 9(3):212-221. https://doi.org/10.9734/BJAST/2015/18148
27. Okwuashi OHS. The Application of Geographic Information Systems Cellular Automata Based Models to Land Use Change Modelling of Lagos, Nigeria. Unpublished PhD Thesis Victoria University of Wellington, 2011.
28. Ozturk D. Urban Growth Simulation of Atakum (Samsun, Turkey) Using Cellular Automata-Markov Chain and Multi-Layer Perceptron-Markov Chain Models. Remote Sensing, 2015, 2015(7). https://doi.org/10.3390/rs70505918
29. Padmanaban R, Bhowmik AK, Cabral P, Zamyatin A, Almegdadi O, Wang S. *et al*. Modelling Urban Sprawl Using Remotely Sensed Data : A Case Study of Chennai City, Tamilnadu. Entropy. 2017; 19(163):1-14. https://doi.org/10.3390/e19040163
30. Raziq A, Xu A, Li Y, Zhao Q. Journal of Remote Sensing & GIS Monitoring of Land Use / Land Cover Changes and Urban Sprawl in Peshawar City in Khyber Pakhtunkhwa : An Application of Geo- Information Techniques Using of Multi-Temporal Satellite Data. Journal of Remote Sensing and GIS. 2016; 5(4):1-11. https://doi.org/10.4172/2469-4134.1000174
31. Richards JA, Jia X. Remote Sensing Digital Image Analysis. New York: Springer, 2006.
32. Rimal B, Zhang L, Keshtkar H, Wang N, Lin Y. Monitoring and Modeling of Spatiotemporal Urban Expansion and Land-Use / Land-Cover Change Using Integrated Markov Chain Cellular Automata Model. ISPRS International Journal of Geo-Information. 2017; 6(288):1-21. https://doi.org/10.3390/ijgi6090288
33. Saifullah K, Barus B, Rustiadi E. Spatial modelling of land use / cover change (LUCC) in South Tangerang City, Banten. IOP Conference Series: Earth and Environmental Science. 2017; 54(1):1-12. https://doi.org/10.1088/1742-6596/755/1/011001
34. Siddhartho SP. Analysis of land use and land cover change in kiskatinaw river watershed: a remote sensing, gis & modeling approach. Unpublished Master Thesis University of Northern British Columbia, 2013.
35. UN. World Urbanization Prospects: The 2014 Revision, Highlights. Department of Economic and Social Affairs ST/ESA/SER.A/352 United Nations, 2014.
36. Wang J, Maduako IN. Spatio-temporal urban growth dynamics of Lagos Metropolitan Region of Nigeria based on Hybrid methods for LULC modeling and prediction Spatio-temporal urban growth dynamics of Lagos Metropolitan Region of. European Journal of Remote Sensing. 2018; 51(1):251-265. https://doi.org/10.1080/22797254.2017.1419831
37. Xie Y, Fan S. Multi-city sustainable regional urban growth simulation-MSRUGS: A case study along the mid-section of Silk Road of China. Stochastic Environmental Research and Risk Assessment. 2014; 28(4):829-841. https://doi.org/10.1007/s00477-012-0680-z
38. Zhang X. Urban Growth Modeling Using Neural Network Simulation: A Case Study of. Journal of Geographic Information System. 2016; (8):317-328.
39. Zhou W, Zhang S, Yu W, Wang J, Wang W. Effects of urban expansion on forest loss and fragmentation in six megaregions, China, 2017. Remote Sensing. https://doi.org/10.3390/rs9100991